Interplay between the Keto Defect and the Interchain Interaction on the Green Emission of Fluorene-Based Polymer

Yi-Shi Wu,[†] Jing Li,[§] Xi-Cheng Ai,[‡] Li-Min Fu,[‡] Jian-Ping Zhang,*[,‡] Ya-Qin Fu,[§] Jian-Jun Zhou,[§] Lin Li,[§] and Zhi-Shan Bo*[,§]

Beijing National Laboratory for Molecular Science (BNLMS), State Key Laboratory for Structural Chemistry of Unstable and Stable Species, State Key Laboratory of Polymer Physics and Chemistry, Institute of Chemistry, Chinese Academy of Sciences, Beijing, 100080, People's Republic of China, and Department of Chemistry, Renmin University of China, Beijing 1000872, People's Republic of China

Received: April 23, 2007; In Final Form: August 23, 2007

To investigate the interplay between on-chain keto defect and interchain interaction and its consequence on the blue emission of polyfluorene (PF), first- to third-generation dendronized PFs as well as single-fluorenone-unit doped PF (PFN), synthesized by Suzuki polycondensation, were used as model compounds for steady-state and picosecond time-resolved photoluminescence (PL) spectroscopic studies. For PF film, the broad-band green emission did not appear, although severe interchain interaction was observed. For PFN film, the green emission that peaked at ∼540 nm decayed in a multiphasic manner, suggesting significant heterogeneity in the excitation migration toward the keto center. To further examine the interplay effect, a series of novel dendronized-PF/PFN blend films in a molar ratio of 40:1 fluorene-to-fluorenone unit were studied. With reference to pure PFN film, those of the green emission of the blends showed strong dependence on the order of dendronization, that is, a higher generation resulted in a shorter-lived green emission. These observations are discussed in terms of interchain and/or intersegment interactions between the fluorene segments and the keto defect. It is concluded that the keto unit and the keto-centered, interchain aggregation lead to severe color degradation in a synergistic manner, and that dendronization can effectively minimize the undesirable green emission.

1. Introduction

Fluorene-based homo- and heteropolymer films constitute an important class of large band gap materials with rather high photoluminescence (PL) quantum yields at blue wavelengths.[1−5] They exhibit high stability against thermal oxidation, good solubility in organic solvents and, therefore, are of great application potentials as the blue-emitting material for organic light-emitting diode,[6−8] as the host material for internal color conversion,[9−11] in liquid crystallinity,[12,13] and in optical switching,[14] etc. However, polyfluorene film encounters the problem of color degradation during device operation or material annealing, that is, the appearance of a broad-band green emission peaked at ∼540 nm (hereafter, referred to as the g-band).[1,15,16] This g-band emission also results in the reduction of the quantum efficiency of blue emission owing to the quenching of electronic excitation of polyfluorene backbone.

Previously, researchers were mainly concentrated on the aggregation and/or interchain excimer formed in polyfluorene films concerning g-band emission.[12,16−20] Recent extensive studies suggest that it originates from the on-chain keto defect introduced by electro-oxidation of the backbone of polyfluorene that may occur during synthesis or device operation processes.[21−31] Most recently, a linear correlation was observed between the relative g-band intensity and the concentration of the keto defect in *dilute* solution, which favors the monomolecular origin of the g-band.[32] Furthermore, theoretical studies of fluorenone-containing oligofluorenes have revealed strong exciton confinement on the fluorenone moieties that may trap the effective electronic excitation of polyfluorene.[24,33] This mechanism readily accounts for the appearance of strong g-band emission for fluorene−fluorenone copolymer with small fraction of fluorenone moieties.

Besides the aforementioned intrachain electronic interactions, the microscopic structure of polyfluorene film is also crucial for the g-band emission. It is first reported that the g-band emission was substantially suppressed by matrix-isolation of the fluorenone-containing polyfluorene chain.[34] In addition, a correlation between the microscopic morphology of fluorene-based polymer and the g-band emission was observed with the help of atomic force microscopy, i.e., the highly organized structure resulted in significant g-band emission, whereas the nonorganized structure retained pure blue emission.[30] Polymer dendronization, which has been successful in fabricating molecular wires and light-emitting materials,[35−38] is a powerful means in isolating the site electronic excitation of the conjugated polymer and in preventing the electronic interaction between the adjacent chains. Accordingly, dendronized polyfluorene had been synthesized and used for blue-emitting materials by several groups.[4,39−41] In an effort to stabilize the blue emission and to avoid the g-band emission, replacing the vulnerable C-9 atom in the polyfluorene backbone by a heteroatom, silicon, was found to be remarkably effective.[42] Most recent investigations

* To whom correspondence should be addressed. Tel: +86-10-62516604. Fax: +86-10-62516444. E-mail: jpzhang@iccas.ac.cn (J.-P.Z.); zsbo@iccas.ac.cn (Z.-S.B.).

[†] State Key Laboratory for Structural Chemistry of Unstable and Stable Species, Chinese Academy of Sciences.

[‡] Renmin University of China.

[§] State Key Laboratory of Polymer Physics and Chemistry, Chinese Academy of Sciences.

10.1021/jp073115z CCC: $37.00
Published on Web 10/16/2007

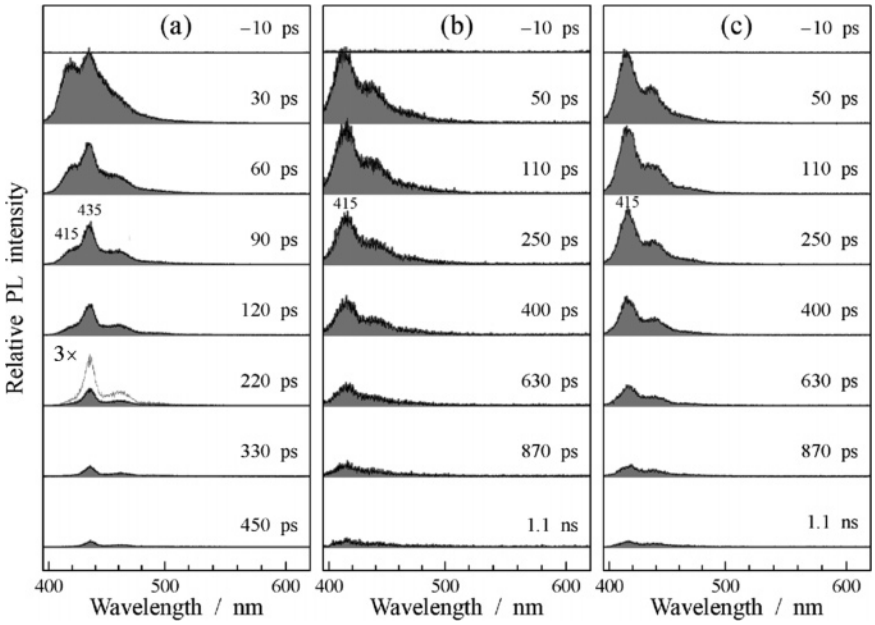

Figure 1. Time-resolved PL spectra at indicated delay times (a) for PF film and for PF in THF solutions; (b) at 1×10^{-5} mol·L^{-1}; and (c) at 1×10^{-3} mol·L^{-1}. Peak wavelengths of the key PL features are labeled. The gate widths at individual delay time are 10, 20, and 20 ps, respectively, for (a), (b), and (c).

SCHEME 1: The Synthetic Route of PFN

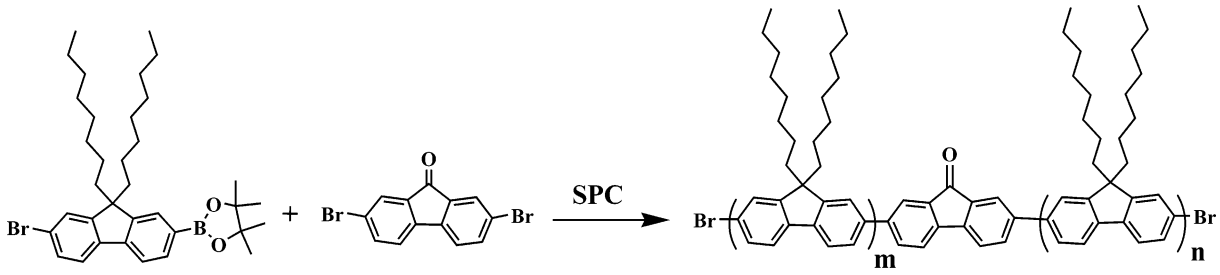

1 **2** **PFN**

m + n = 20

on the electro- and photoluminescence characters of polyfluorene-based copolymers adopting quinoxaline or dibenzo[*a*,*c*]-phenazine as the building blocks have proved that optimization of the composition and introduction of the intramolecular charge-transfer excited states are effective approaches in improving the electroluminescence performance of the blue emitting copolymers, for example, thermal oxidative stability and external quantum efficiency.[43,44]

Despite the general agreement of the keto-defect origin of the g-band emission in polyfluorene, it is strongly argued that the interchain/intersegment interactions are required for the appearance of the g-band for which the oxidation-induced fluorenone defect alone is not sufficient.[45−47] The present work has been attempted to investigate the effect of on-chain keto defect and that of interchain interaction on the g-band emission with an emphasis on their interplay. For this purpose, well-defined polymers 9,9-dioctyl-polyfluorene (PF), free from keto defect, and poly-(9,9-dioctylfluorene)s-*co*-fluorenone (PFN), containing a single fluorenone unit, were synthesized and adopted as the model compounds. In addition, first- to third-generation dendronized PFs (PFg1, PFg2, and PFg3) were employed to regulate the site isolation of electronic excitation in the PF/PFN blend films with well-controlled fluorene-to-fluorenone stoichiometry. The photophysics of PF, PFN, and their blends, either in solution or in film, were examined by means of steady-state and picosecond time-resolved PL spectroscopies.

2. Experimental Methods

Sample Preparation. PF and PFg1∼3 were synthesized by the Suzuki polycondensation (SPC) following a reported procedure.[41] The synthetic route for PFN is briefly described below (Scheme 1). One-pot SPC of 7-bromo-9,9-dioctylfluorene-2-boronic ester (1) with 2,7-dibromo-fluorenone (2) in a molar ratio of 20:1 under standard conditions afforded the desired polymer PFN in a 78% yield with $Pd(PPh_3)_4$ as a catalyst precursor. The structure of PFN was characterized unambiguously with ^{1}H and ^{13}C NMR spectroscopy and combustion analysis. Chart 1 depicts the molecular structures of nondendronized 9,9-dioctyl-polyfluorene (PF), the first-generation dendronized PF (PFg1), the second-generation dendronized PF (PFg2), and third-generation dendronized PF (PFg3), as well as the poly-(9,9-dioctylfluorene)s-*co*-fluorenone (PFN). Gel permeation chromatography of PF, PFg1, PFg2, and PFg3 showed the number-average degree of polymerization 25, 47, 78, and 47, respectively. The apparent weight- and the number-average molecular weights (Mw and Mn) of PFN were found to be 101 500 and 35 800, respectively. Each PFN chain contains ∼20 fluorene units and only one fluorenone unit. To prepare

CHART 1: The Chemical Structures of PF, PFN, and Dendronized PFs (PFg1, PFg2, and PFg3)

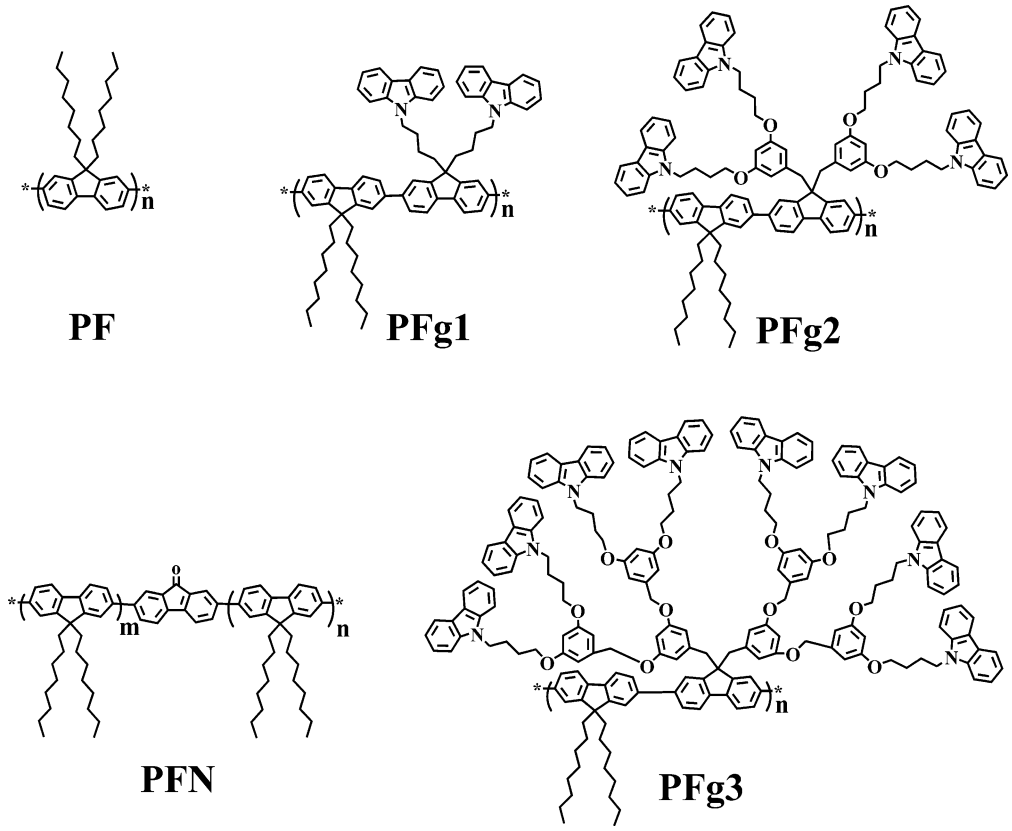

casting films for spectroscopic measurements, PFs or PFN were dissolved in tetrahydrofuran (THF) in a concentration of 1×10^{-3} mol·L^{-1} for the fluorene unit, which were subjected to spin-coating. The same mother solution was used to obtain the diluted solution at a desired concentration.

Steady-State and Time-Resolved PL Spectroscopies. Steady-state PL measurement was carried out on a fluorescence spectrophotometer (F-2500, Hitachi). To suppress the effect of self-absorption, a quartz cell of 1 mm optical path length was used with its normal forming 45° with reference to the actinic and the luminescence light beams. The excitation wavelength was 377 nm, and the spectral bandwidth for either the excitation or the detection was 2.5 nm.

The excitation laser pulses (377 nm) for the picosecond time-resolved PL experiment were supplied by an optical parametric amplifier (OPA-800CF, Spectra Physics), which was pumped by the output from a regenerative amplifier (Spitfire, Spectra Physics). The excitation pulse energy was ∼100 nJ/pulse. Fluorescence collected with the 180° geometry was dispersed by a polychromator (250is, Chromex) and detected with a photon-counting type streak camera (C2909, Hamamatsu Photonics). The spectral resolution was 0.2 nm, and the temporal resolution was 20∼100 ps depending on the delay time-range setting. All the spectroscopic measurements were carried out at room temperature.

3. Results and Discussion

We first examine the spectral dynamics of the picosecond time-resolved luminescence spectra shown in Figure 1. Immediately following the pulsed excitation at 377 nm, PF film exhibits broad-band emission in the range of 400∼520 nm with two distinct peaks at 415 and 435 nm, respectively (Figure 1a). The 415 nm peak decays out completely at ∼220 ps, whereas the 435 nm band with clear vibronic structures stays. On the other hand, both of the diluted PF solutions (Figure 1b,c) exhibit similar transient spectra in the range of 400∼500 nm, and their vibronic features do not show any time-dependent changes. The spectral dynamics for the cases of higher (1×10^{-3} mol·L^{-1}) and lower (1×10^{-5} mol·L^{-1}) concentrations are quite similar, however, the decay time constants are slightly longer at higher concentration (Table 1), which may be an indication of the formation of aggregation.[30,48] Nevertheless, it is safe to conclude that the interchain aggregation was negligible at a concentration as low as 1×10^{-5} mol·L^{-1}.

The steady-state PL spectra of PF either in film (Figure 2a) or in solution (Figure 2b) show no recognizable g-band emission peaked at ∼540 nm and extending over 600 nm, a fact that proves our nondendronized PF was free from keto defect. The spectrum integrated over the entire delay time range of −0.1∼1.1 ns for PF solution agrees well with the steady-state spectrum, however, that for PF film differs significantly from the steady-state one, indicating the existence of transient PL components lived beyond the window of integration time.

The PL spectrum of PF in solution is characterized by three well-resolved vibronic bands peaked at 415 (0→0), 440 (0→1), and 473 nm (0→2) with an average vibronic separation of ∼1480 cm^{-1}. The PL kinetics of the vibronic bands can be fit nicely to a single-exponential decay model function with a decay time constant of ∼0.4 ns (Figure 2d, Table 1), suggesting that the amount of PF aggregation is negligible at the concentration of 1×10^{-5} mol·L^{-1}. For PF film, on the other hand, both steady-state and time-integrated PL spectra show vibronic features at 415, 435, 460, and 494 nm; the apparent decay time constant of the 415 nm band, 0.04 ns, is much shorter than those of the other three (0.18∼0.23 ns (Figure 2c, Table 1)). The nonexponential kinetic behavior of PF film reflects the dispersive relaxation dynamics in the electronic excitation transfer processes.[49,50] The 435, 460, and 494 nm bands shifted systemati-

TABLE 1: Apparent Decay Time Constants for the THF Solution and the Casting Film of PF and PFN as Derived from the PL Kinetics in Figures 2 and 4

sample description	decay time constant (ns)			
PF in THF	415 nm (0→0)	440 nm (0→1)	473 nm (0→2)	
1×10^{-5} mol·L^{-1}	0.41 ± 0.01	0.38 ± 0.01	0.40 ± 0.01	
1×10^{-3} mol·L^{-1}	0.40 ± 0.01	0.42 ± 0.01	0.46 ± 0.01	
PF film[a]	416 nm	435 nm (0→0)	460 nm (0→1)	494 nm (0→2)
	~0.04	0.18	0.21	0.23
PFN in THF	419 nm	555 nm	570 nm	
1×10^{-5} mol·L^{-1}	0.42 ± 0.01	3.6 ± 0.1	3.9 ± 0.1	
PFN film[a]	419 nm	555 nm	570 nm	
	~0.03	4.52	4.66	

[a] Nonexponential decay for which an apparent decay time constant $<\tau>$ was determined by using the relation[51] $\langle\tau\rangle = \sum_{i=1}^{n} a_i\tau_i^2/a_i\tau_i$ ($n = 2\sim3$), where τ_i and a_i, respectively, represent the individual exponential decay time constant and the corresponding preexponential factor.

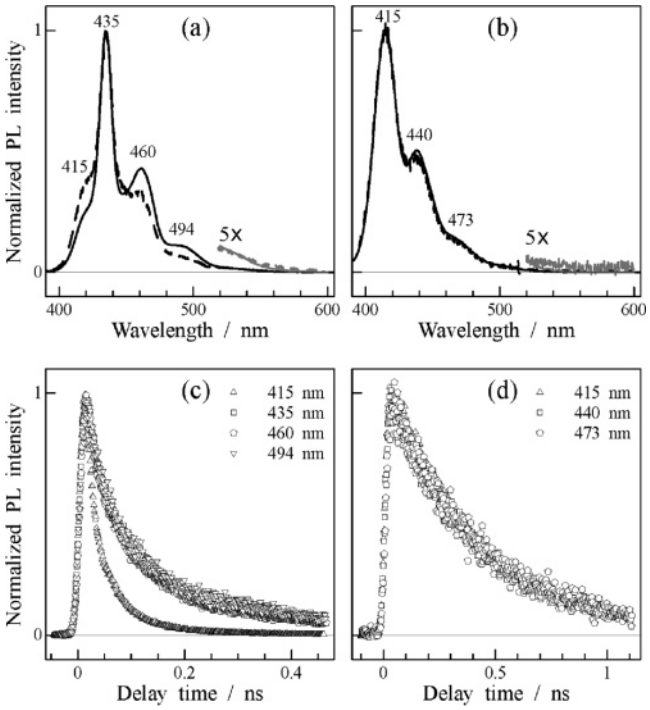

Figure 2. Steady-state (solid line) and time-integrated (dashed line) PL spectra of PF (a) in film and (b) in THF solution at 1×10^{-5} mol·L^{-1}. (c−d) These present the PL kinetics at indicated probe wavelengths corresponding to the cases (a) and (b), respectively.

cally to the longer wavelength side for ~20 nm with respect to the PF solution, which is consistent with a recent observation of a 22 nm red shift of vibronic bands for poly(2,7-fluorene ethynylene) film.[52] With reference to PF in diluted solution, a red shift of 15~20 nm is typical for its aggregation in solid,[34] therefore, we ascribe the three longer wavelength bands to vibronic emissions from the same excitonic state of PF aggregation (Table 1). Because no decay-to-rise correlation has been found between the 415 nm kinetics and the other longer-lived kinetics, the 415 nm peak PL component may originate from the isolated excitation of PF segment that has undergone rapid equilibration among the on-chain and/or interchain adjacent PF segments.

PL Spectroscopy of PFN Solution and Film. Fluorenone-unit-implanted polyfluorene is a useful model compound in elucidating the photophysical mechanism of color degradation.[28−31] We have made use of the PFN copolymer containing a single keto unit to mimic the photophysical properties of photo-oxidized PF.

As shown in Figure 3, steady-state PL spectra of PFN solutions exhibit a blue emission originated from polymeric fluorene (400~500 nm) along with the g-band from the keto unit (500~700 nm). We have normalized the luminescence spectra at the peak wavelength of 0→1 vibronic transition of blue emission; the 0→0 vibronic band was not chosen for normalization because it was distorted by the self-absorption at higher PFN concentration. In this way, the influence of absolute PFN concentration on the g-band intensity can be removed, and the change in intensity can be regarded as mainly induced by the interchain interaction between PFN chains. It is seen for PFN solution that the g-band emission enhances considerably upon increasing the concentration from 1×10^{-8} to 1×10^{-3} mol·L^{-1}, which is in agreement with Kulkarni and coauthors' recent observation on the fluorene−fluorenone copolymers.[31] Note that the g-band intensity increases linearly up to 1×10^{-4} mol·L^{-1} and intends to saturate at higher concentrations (Figure 3b). The linear correlation between the intensity of g-band and the concentration of PFN in dilute solution indicates the monomolecular origin of g-band, consistent with the proposal of Lupton et al.[32] Because the ground-state absorption spectrum of PFN film vanishes beyond 450 nm, self-absorption in the spectral region of g-band emission can be neglected; therefore, the PL saturation at the concentration higher than 1×10^{-4} mol·L^{-1} may be due to the reduction in luminescence quantum yield induced by the existence of densely packed PFN chains, that is, PFN aggregate. Compared to fluorene, the fluorenone unit is indeed more planar, has less steric hindrance, and hence is much easier to form aggregation with the effective fluorene unit in close proximity.[31,53]

In the case of PFN film, the g-band pattern is almost the same as that of the PFN solution (1×10^{-3} mol·L^{-1}), and its intensity overwhelms the blue emission (see Figure 3a and its inset). The drastic reduction in blue emission with reference to PFN solution is due to the keto unit that acts as an efficient trap of the effective fluorene excitations among the densely packed PFN chains.[24,33] The nearly unchanged g-band pattern between the PFN film and solutions is not in consistent with the fluorenone-based-excimer origin of the g-band.[45]

It is seen from Figure 3a that the g-band persists even at extremely low concentration (1×10^{-8} mol·L^{-1}), and that the increase in the relative intensity of g-band emission upon increasing PFN concentration is obvious but not significant. On the other hand, for the casting film of pure PF, no g-band emission appeared despite the clear spectral indication of PF aggregation (vide supra). Taken together it seems that while the keto center is essential for the g-band to appear, the interchain interactions are absolutely needed for the overwhelming g-band. Here, we would like to stress that the keto unit and the interchain interaction in PFN film contribute to the g-band emission in a synergistic manner: Neither merely interchain interaction between the effective PF segments nor on-chain keto defect alone can induce the overwhelmingly intense g-band in

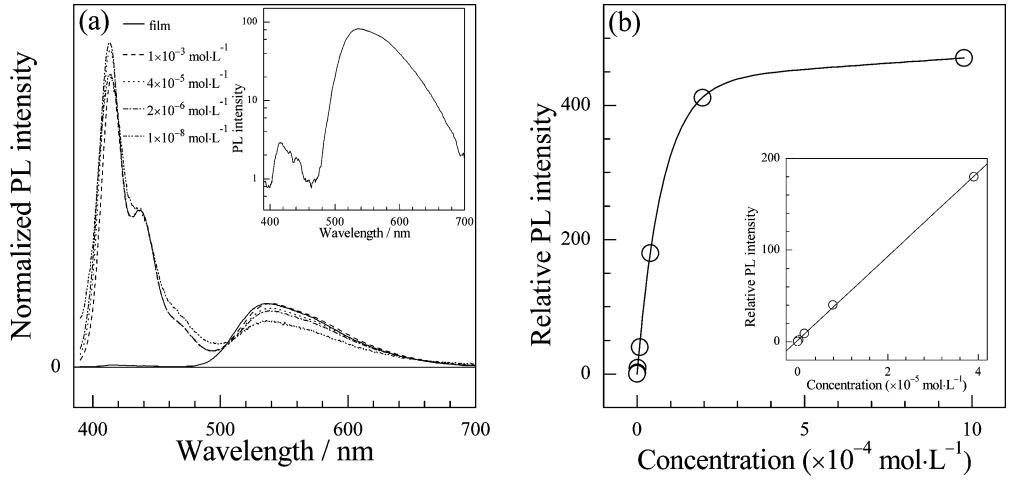

Figure 3. (a) Steady-state PL spectra for PFN film and for its THF solutions at indicated concentrations; spectra are normalized to the 0→1 vibronic band of the blue emission. The spectrum of PFN film is normalized to the g-band of PFN solution at 1×10^{-3} mol·L^{-1}, and the inset shows its details. (b) Concentration dependence of the g-band intensity at 535 nm.

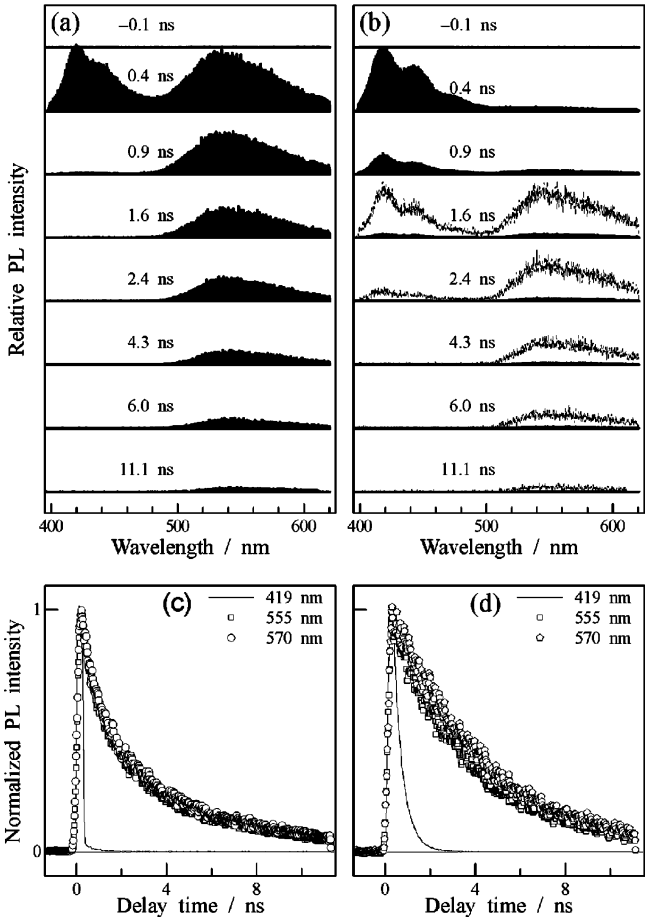

Figure 4. Time-resolved PL spectra at the indicated delay times for (a) PFN film and (b) PFN in THF solution at 1×10^{-5} mol·L^{-1}. Light gray lines in (b) are blow-up spectra (×7). The width of time-gate is 240 ps for each transient. (c−d) These graphs show the PL kinetics at indicated wavelengths directly plotted, respectively, from (a) and (b).

the film of fluorene-based polymer, it is their interplay that results in the severe color degradation. This implicitly means that the keto-unit-involved aggregation structure is responsible for the intense g-band.

The 0.4 ns transient in Figure 4a shows that for PFN film the fluorene-based blue emission and the fluorenone-based green one are equally intense. The blue emission decays out completely within a nanosecond, whereas the g-band lasts until ∼11 ns. The energy migration from the fluorene segment to the fluorenone center takes place within the limit of the time resolution (Figure 4c), that is, the interchain aggregation of PFN leads to extremely fast energy equilibration before the excitonic state for g-band emission starting to depopulate. Because of the efficient flow of excitation energy to the fluorenone site, the decay time constant of blue emission (∼0.03 ns) is significantly shorter than that of PF film (0.18∼0.23 ns, Table 1), whereas the g-band emission exhibits a much longer lifetime (4.52∼4.66 ns) which is due to the weakly allowed CT $\pi-\pi^*$ transition of fluorenone.[24,54]

It is seen from Figure 4c,d that the 419 nm kinetics of PFN film decays much faster than that of PFN solution (0.03 ps versus ∼0.4 ns, Table 1), which is understandable in view of the third- versus first-dimensional migration of excitation to the fluorenone site in film and in diluted solution, respectively.[31] Compared to PFN film, the 10-fold longer-lived blue emission of PFN in diluted solution implies that the on-chain fluorene-to-fluorenone excitation energy transfer (EET) is much less efficient than the interchain EET, which is consistent with the result of a recent theoretical prediction.[55] This also implicitly means that the fluorene−fluorenone interaction between different chains is much stronger than that in the same backbone. In addition, the g-band emission of PFN film shows a nonexponential decay, whereas that of the PFN solution obeys simple single-exponential behavior, suggesting the existence of more than one emitting species in a sense that different aggregation forms may exist in the PFN film. For example, the 570 nm kinetics in Figure 4c could be best accounted for by a three-exponential-decay model, which resulted in the apparent time constants of 0.2 ± 0.1, 1.2 ± 0.3, and 5.5 ± 0.6 ns with the relative prefactors of 40, 31, and 29%, respectively. We ascribe the longest-lived component (5.5 ± 0.6 ns), contributing ∼29% to the total emission intensity, to the monomeric fluorenone species because its lifetime is comparable to that of PFN in solution (3.9 ± 0.1 ns, Table 1). Whereas the emitting species for the other two time scales are unclear, their collective contribution of 71% indicates the large inhomogeneity of the g-emission processes. In this context, the nonexponential character of g-emission kinetics had been explained in terms of dispersive electronic excitation transfer,[49,50] that is, the downhill excitation transfer processes in solid-state material among the adjacent structures having different energy levels. The nonexponential character of the g-band kinetics for the PFN

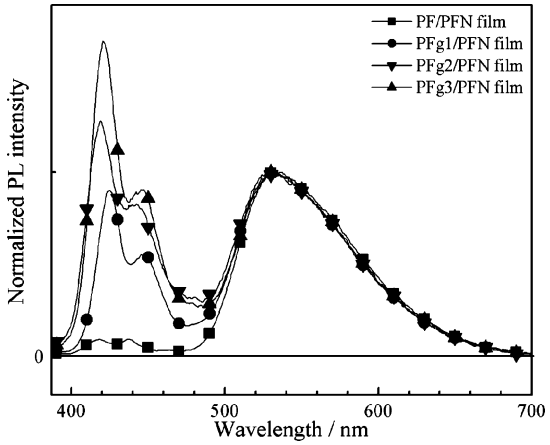

Figure 5. Steady-state PL spectra of dendronized-PF/PFN blend films normalized to the peak wavelength of the g-band.

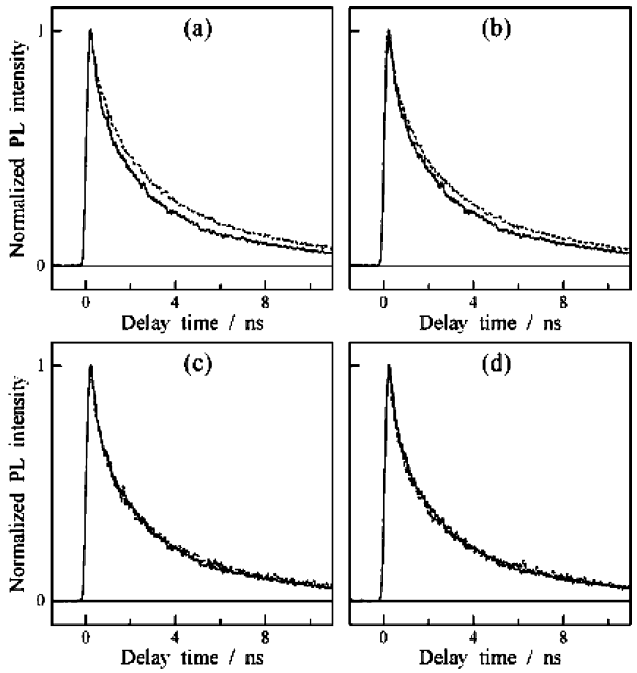

Figure 6. Normalized g-band kinetics at 570 nm for blend films of (a) PF/PFN, (b) PFg1/PFN, (c) PFg2/PFN, and (d) PFg3/PFN (dashed line) with an overall fluorene-to-fluorenone molar ratio of 40:1. The g-band kinetics of pure PFN film (solid line) is shown for comparison.

copolymer film is contradictory to the recent work by Kulkarni et al. who reported simple single-exponential kinetics and claimed that on-chain monomeric fluorenone defect results in the generation of g-band.[31] This discrepancy may result from the improved temporal resolution in our work (~0.1 ns) with respect to that in ref 31(a few nanoseconds).

Fluorenone-Centered Aggregation Enhances the G-Band Emission. As demonstrated above, the interplay between the keto defect and the PFN−PFN and/or PFN−PF interchain interactions significantly enhances the g-band emission. It is also known that dendronization is effective and widely adopted in controlling the intermolecular interaction between polymeric chains.[39,56−58] We have made use of the dendronized-PF/PFN blend films, consisting of an overall fluorene-to-fluorenone molar ratio of 40:1, to further investigate the interplay and, more importantly, to seek for a solution in minimizing the g-band emission.

It is clearly seen from Figure 5 that, upon increasing the generation of dendronization, the relative intensity of blue emission of the blend film increases significantly, proving that dendronization can stabilize the blue emission effectively. From PF to PFg3, the blue band is enhanced; however, no further improvement is seen from the PFg2 blend film to the PFg3 one. This implies that dendronization exceeding two-generation may be no more effective for improving the color stability.

Figure 6 shows the g-band kinetics of these model blends, which are plotted at the red side of the g-band (570 nm) so as to avoid the possible interference from the fluorene-origin blue emission. It is obvious that the g-band kinetics for different blends is all nonexponential, and that mixing up PFN with a higher-generation dendronized PF leads to a shorter-lived g-band emission. The g-band emission in blend films must originate from the ketonic unit in PFN, because the dendronized-PF films without PFN show no g-band characteristics in the spectral range of g-band. For the aforementioned PFN film, energy migration from fluorene segment to fluorenone center takes place within the limit of the time resolution (Figure 4c), that is, the PFN−PFN aggregation leads to energy equilibration before the depopulation of the low-energy state for the g-band emission and, therefore, does not affect the relatively long-lived g-band kinetics. The decrease in the g-band lifetime upon increasing the generation of dendronization is attributable to a weaker dendronized-PF/PFN interchain interaction owing to the increasingly large molecular separation. Most importantly, this result proves that dendronization can effectively minimize the undesired g-band emission.

It is interesting to see that the model blends involving higher generation of dendronization, PFg2/PFN and PFg3/PFN, show nearly the same kinetics as pure PFN film. This phenomenon can be interpreted that dendronization as high as second-generation is sufficiently effective in controlling the interchain interaction of fluorene-based polymers, consistent with the result of steady-state PL measurement.

4. Conclusions

To investigate the interplay between on-chain keto defect and the interchain aggregation on the undesired g-band emission of the fluorene-based, blue-emitting polymers, we have synthesized PF dendronized with three successive generations (PFg1~3), as well as that doped with a single fluorenone unit (PFN). These model compounds were subjected to steady-state and picosecond time-resolved photoluminescence spectroscopic studies. For pure PF film, severe interchain interactions were observed but no green emission appeared. The pure PFN film showed a multiphasic-decayed g-band emission, suggesting the heterogeneous excitation migration processes and the significant contribution from the interchain interaction. To further examine the interplay effect on the g-band emission, we have examined a series of novel dendronized-PF/PFN blend films in a fluorene-to-fluorenone unit molar ratio of 40:1. The apparent lifetimes of the g-band emission of PFg1~3 blend films showed strong dependence on the order of PF-dendronization, that is, a higher generation of dendronization correlates to a shorter-lived g-band emission. The results above are discussed in terms of interchain and/or intersegment interactions between PF and PFN segments and the excitation trapping effect of the keto center.

Our results prove that the aggregation-enhanced electronic interaction and the keto defect degrade the blue emission of PF film in a synergistic manner, that is, their interplay causes much stronger g-band emission than the sum of individual consequences. It is the keto-centered interchain aggregation and/or intersegment interaction that play a crucial role in this color degradation. Furthermore, we show that, while the chemical

defect may be avoided by improving the synthesis and the film preparation protocols, the g-band emission cannot be completely eliminated merely by site isolation of the effective fluorene excitation. However, it is unambiguously demonstrated that dendronization is indeed effective in minimizing the undesirable g-band emission and at the same time in stabilizing the blue emission of PF film.

Acknowledgment. This work has been sponsored by the Natural Science Foundation of China (Grants 20673144 and 20433010) and by the Major State Basic Research Development Program (Grant 2002CB613401). Financial support from the Knowledge Innovation Projects of the Chinese Academy of Sciences is also acknowledged.

References and Notes

(1) Pei, Q.; Yang, Y. *J. Am. Chem. Soc.* **1996**, *118*, 7416.
(2) Ranger, M.; Rondeau, D.; Leclerc, M. *Macromolecules* **1997**, *30*, 7686.
(3) Klarner, G.; Davey, M. H.; Chen, W. D.; Scott, J. C.; Miller, R. D. *Adv. Mater.* **1998**, *10*, 993.
(4) Marsitzky, D.; Vestberg, R.; Blainey, P.; Tang, B. T.; Hawker, C. J.; Carter, K. R. *J. Am. Chem. Soc.* **2001**, *123*, 6965.
(5) Xia, C. J.; Advincula, R. C. *Macromolecules* **2001**, *34*, 5854.
(6) Gross, M.; Müller, D. C.; Nothofer, H.-G.; Scherf, U.; Neher, D.; Bräuchle, C.; Meerholz, K. *Nature* **2000**, *405*, 661.
(7) Grice, A. W.; Bradley, D. D. C.; Bernius, M. T.; Inbasekaran, M.; Wu, W. W.; Woo, E. P. *Appl. Phys. Lett.* **1998**, *73*, 629.
(8) Friend, R. H.; Gymer, R. W.; Holmes, A. B.; Burroughes, J. H.; Marks, R. N.; Taliani, C.; Bradley, D. D. C.; Dos-Santos, D. A.; Brédas, J. L.; Lögdlund, M.; Salaneck, W. R. *Nature* **1999**, *397*, 121.
(9) Virgili, T.; Lidzey, D. G.; Bradley, D. D. C. *Adv. Mater.* **200**0, *12*, 58.
(10) Lane, P. A.; Palilis, L. C.; O'Brien, D. F.; Giebeler, C.; Cadby, A. J.; Lidzey, D. G.; Campbell, A. J.; Blau, W.; Bradley, D. D. C. *Phys. Rev. B* **2001**, *63*, 235206.
(11) Li, B. S.; Li, J.; Fu, Y. Q.; Bo, Z. S. *J. Am. Chem. Soc.* **2004**, *126*, 3430.
(12) Teetsov, J.; Fox, M. A. *J. Mater. Chem.* **1999**, *9*, 2117.
(13) Grell, M.; Knoll, W.; Lupo, D.; Meisel, A.; Miteva, T.; Neher, D.; Nothofer, H. G.; Scherf, U.; Yasuda, A. *Adv. Mater.* **1999**, *11*, 671.
(14) Virgili, T.; Marinotto, D.; Lanzani, G.; Bradley, D. D. C. *Appl. Phys. Lett.* **2005**, *86*, 091113.
(15) Long, X.; Grell, M.; Malinowski, A.; Bradley, D. D. C.; Inbasekaran, M.; Woo, E. P. *Opt. Mater.* **1998**, *9*, 70.
(16) Bliznyuk, V. N.; Carter, S. A.; Scott, J. C.; Klärner, G.; Miller, R. D.; Miller, D. C. *Macromolecules* **1999**, *32*, 361.
(17) Herz, L. M.; Phillips, R. T. *Phys. Rev. B* **2000**, *61*, 13691.
(18) Li, J.; Li, Z.; Zhan, C. M.; Qin, J. G.; Li, Y. L. *Synth. Met.* **1999**, *101*, 127.
(19) Teetsov, J. A.; Vanden Bout, D. A. *J. Am. Chem. Soc.* **2001**, *123*, 3605.
(20) Zeng, G.; Yu, W. L; Chua, S. J.; Huang, W. *Macromolecules* **2002**, *35*, 6907.
(21) Gong, X.; Moses, D.; Heeger, A. J.; Xiao, S. *Synth. Met.* **2004**, *141*, 17.
(22) Lupton, J. M.; Craig, M. R.; Meijer, E. W. *Appl. Phys. Lett.* **2002**, *80*, 4489.
(23) List, E. J. W.; Guentner, R.; Scandiucci de Freitas, P.; Scherf, U. *Adv. Mater.* **2002**, *14*, 374.
(24) Zojer, E.; Pogantsch, A.; Hennebicq, E.; Beljonne, D.; Brédas, J. L.; Scandiucci de Freitas, P.; Scherf, U.; List, E. J. W. *J. Chem. Phys.* **2002**, *117*, 6794.
(25) Scherf, U.; List, E. J. W. *Adv. Mater.* **2002**, *14*, 477.
(26) Gong, X.; Iyer, P. K.; Moses, D.; Bazan, G. C.; Heeger, A. J.; Xiao, S. S. *Adv. Funct. Mater.* **2003**, *13*, 325.
(27) Craig, M. R.; de Kok, M. M.; Hofstraat, J. W.; Schenning, A. P. H. J.; Meijer, E. W. *J. Mater. Chem.* **2003**, *13*, 2861.
(28) Romaner, L.; Pogantsch, A.; Scandiucci de Freitas, P.; Scherf, U.; Gaal, M.; Zojer, E.; List, E. J. W. *Adv. Funct. Mater.* **2003**, *13*, 597.
(29) Gaal, M.; List, E. J. W.; Scherf, U. *Macromolecules* **2003**, *36*, 4236.
(30) Surin, M.; Hennebicq, E.; Ego, C.; Marsitzky, D.; Grimsdale, A. C.; Müllen, K.; Brédas, J. L.; Lazzaroni, R.; Leclère, P. *Chem. Mater.* **2004**, *16*, 994.
(31) Kulkarni, A. P.; Kong, X. X.; Jenekhe, S. A. *J. Phys. Chem. B* **2004**, *108*, 8689.
(32) Becker, K.; Lupton, J. M.; Feldmann, J.; Nehls, B. S.; Galbrecht, F.; Gao, D. Q.; Scherf, U. *Adv. Funct. Mater.* **2006**, *16*, 364.
(33) Franco, I.; Tretiak, S. *Chem. Phys. Lett.* **2003**, *372*, 403.
(34) Kulkarni, A. P.; Jenekhe, S. A. *Macromolecules* **2003**, *36*, 5285.
(35) Schenning, A. P. H. J.; Martin, R. E.; Ito, M.; Diederich, F.; Boudon, C.; Gisselbrecht, J. P.; Gross, M. *Chem. Commun.* **1998**, *9*, 1013.
(36) Kaneko, T.; Horie, T.; Asano, M.; Aoki, T.; Oikawa, E. *Macromolecules* **1997**, *30*, 3118.
(37) Sato, T.; Jiang, D. L.; Aida, T. *J. Am. Chem. Soc.* **1999**, *121*, 10658.
(38) Schlüter, A. D.; Rabe, J. P. *Angew. Chem., Int. Ed.* **2000**, *39*, 864.
(39) Setayesh, S.; Grimsdale, A. C.; Weil, T.; Enkelmann, V.; Müllen, K.; Meghdadi, F.; List, E. J. W.; Leising, G. *J. Am. Chem. Soc.* **2001**, *123*, 946.
(40) Chou, C. H.; Shu, C. F. *Macromolecules* **2002**, *35*, 9673.
(41) Fu, Y. Q.; Li, Y.; Li, J.; Yan, S. K.; Bo, Z. S. *Macromolecules*, **2004**, *37*, 6395.
(42) Chan, K. L.; Mckiernan, M. J.; Towns, C. R.; Holmes, A. B. *J. Am. Chem. Soc.* **2005**, *127*, 7662.
(43) Kulkarni, A. P.; Zhu, Y.; Jenekhe, S. A. *Macromolecules* **2005**, *38*, 1553.
(44) Zhu, Y.; Gibbons, K. M.; Kulkarni, A. P.; Jenekhe, S. A. *Macromolecules*, **2007**, *40*, 804.
(45) Sims, M.; Bradley, D. D. C.; Ariu, M.; Koeberg, M.; Asimakis, A.; Grell, M.; Lidzey, D. G. *Adv. Funct. Mater.* **2004**, *14*, 765.
(46) Chochos, C. L.; Kallitsis, J. K.; Gregoriou, V. G. *J. Phys. Chem. B* **2005**, *109*, 8755.
(47) Chen, X. W.; Tseng, H. E.; Liao, J. L.; Chen, S. A. *J. Phys. Chem. B* **2005**, *109*, 17496.
(48) Kim, J.; Swager, T. M. *Nature* **2001**, *411*, 1030.
(49) Meskers, S. C. J.; Hubner, J.; Oestreich, M.; Bässler, H. *Chem. Phys. Lett.* **2001**, *339*, 223.
(50) Meskers, S. C. J.; Hubner, J.; Oestreich, M.; Bässler, H. *J. Phys. Chem. B* **2001**, *105*, 9139.
(51) Neves-Petersen, M. T.; Gryczynski, Z.; Lakowicz, J.; Fojan, P.; Pedersen, S.; Petersen, E.; Petersen, S. B. *Protein Sci.* **2002**, *11*, 588.
(52) Lee, S. H.; Nakamura, T.; Tsutsui, T. *Org. Lett.* **2001**, *3*, 2005.
(53) Panozzo, S.; Vial, J. C.; Kervella, Y.; Stéphan, O. *J. Appl. Phys.* **2002**, *92*, 3495.
(54) Chi, C. Y.; Im, C.; Enkelmann, V.; Ziegler, A.; Lieser, G.; Wegner, G. *Chem.—Eur. J.* **2005**, *11*, 6833.
(55) Beljonne, D.; Pourtois, G.; Silva, C.; Hennebicq, E.; Herz, L. M.; Friend, R. H.; Scholes, G. D.; Setayesh, S.; Müllen, K.; Brédas, J. L. *Proc. Natl. Acad. Sci. U.S.A.* **2002**, *99*, 10982.
(56) Lupton, J. M.; Samuel, I. D. W.; Beavington, R.; Frampton, M. J.; Burn, P. L.; Bässler, H. *Phys. Rev. B* **2001**, *63*, 155206.
(57) Lupton, J. M.; Samuel, I. D. W.; Beavington, R.; Burn, P. L.; Bässler, H. *Adv. Mater.* **2001**, *13*, 258.
(58) Lupton, J. M.; Samuel, I. D. W.; Burn, P. L.; Mukamel, S. *J. Phys. Chem. B* **2002**, *106*, 7647.